Peculiar pathological, radiological and clinical features of skull base dedifferentiated chordomas. Results from a referral Center case series and literature review

DR COSTANTINO RICCI (Orcid ID : 0000-0001-7254-4195)
DR ALBERTO RIGHI (Orcid ID : 0000-0002-1074-0155)

Article type : Original Article

Peculiar pathological, radiological and clinical features of skull base dedifferentiated chordomas. Results from a referral Center case series and literature review

Running title: Case series of skull base dedifferentiated chordomas

Asioli Sofia[1,2,3], Zoli Matteo[2,3], Guaraldi Federica[2,3], Sollini Giacomo[4], Bacci Antonella[5], Gibertoni Dino[6], Ricci Costantino[1], Morandi Luca[1], Pasquini Ernesto[4], Righi Alberto[7], and Mazzatenta Diego[2,3]

1. Section of Anatomic Pathology 'M. Malpighi', Bellaria Hospital, Bologna, Italy.
2. Department of Biomedical and Neuromotor Sciences (DIBINEM), University of Bologna, Bologna, Italy.
3. Pituitary Unit - Center for the Diagnosis and Treatment of Hypothalamic and Pituitary Diseases -, Department of Biomedical and Neuromotor Sciences (DIBINEM) of Neurological Sciences of Bologna, Bologna, Italy.
4. ENT Division, Bellaria Hospital, Bologna, Italy.
5. Division of Neuroradiology, IRCCS Institute of Neurological Sciences of Bologna, Bologna, 40139, Italy.
6. Unit of Hygiene, Public Health and Biostatistics, Department of Biomedical and Neuromotor Sciences, University of Bologna, Italy
7. Service of Anatomic Pathology, IRCCS Istituto Ortopedico Rizzoli, Bologna, Italy.

This article has been accepted for publication and undergone full peer review but has not been through the copyediting, typesetting, pagination and proofreading process, which may lead to differences between this version and the Version of Record. Please cite this article as doi: 10.1111/HIS.14024

Corresponding author:
Dr. Alberto Righi, MD PhD
Service of Anatomic Pathology, IRCCS Istituto Ortopedico Rizzoli.
Via di Barbiano 1/10
I-40137, Bologna, Italy
Telephone (office): +39 051 6366665
Fax (office): + 39 051 6366592
e-mail: alberto.righi@ior.it

Conflict of Interest: The authors declare that they have no conflict of interest.

Word count: 2909

Abstract

Background: Dedifferentiated chordoma is an uncommon and incompletely characterized aggressive neoplasm. Only few cases originating from the skull base have been reported.

Material & methods: All consecutive cases of skull base dedifferentiated chordomas treated surgically in a referral Center from January 1990 to June 2019 were retrospectively evaluated to assess peculiar pathological, radiological and clinical features. Patient data were retrieved from paper and electronic records.

Results: Six cases (4 F; mean age at surgery 46 years, range 35-64), treated surgically at our Institution were identified. Transformation to dedifferentiated chordomas occurred after radiation therapy in 3 cases (mean 13.6 years after treatment, range 5-25), 2 during tumor progression, while one was de-novo. Magnetic resonance imaging and surgical examination revealed the presence of two different tumor components, corresponding to the conventional and dedifferentiated portion at histological examination. The de novo case presented a *PIK3CA* mutation. DNA methylation analysis revealed consistent epigenetic changes in *TERT, MAGEA11* and *UXT*. Prognosis was poor as 5 out of 6 patients died after surgery and radiation therapy, with a mean overall survival of 29 months (range

11-52).

Conclusions: Skull base dedifferentiated chordomas are extremely rare and aggressive neoplasms with characteristic magnetic resonance imaging, surgical and histological features. Therefore, an early and accurate histological diagnosis is of paramount relevance. Molecular analysis appears promising to define mechanisms involved in tumor dedifferentiation.

Key Words: Dedifferentiated chordoma, skull base tumor, bone tumor, endoscopic endonasal surgery, outcome

INTRODUCTION

Chordomas are rare (incidence 0.5-0.8 cases/million people/year) malignant bone tumors originating from notochordal remnants.[1] They typically affect the sacrum (50%-60%) and, less frequently, the skull base (25%-30%) and the vertebrae (15%), while extra-axial localizations have been reported anecdotally.[1-4] Skull base chordomas are typically midline lesions that arise from the clivus and grow

above the McGregor's line.[5-6] Despite the recent advancements of minimally invasive surgery, and the availability of more precise and effective radiation and medical treatments, prognosis of skull base forms remains poor, with a mean overall survival of about 50% at 10 years.[5-6] Tumor histotype seems one of the most important prognostic factors.[5-6] Sarcomatous, poorly differentiated and dedifferentiated variants are rare but extremely aggressive, and represent a challenge for the pathologist.[5-13] Among them, dedifferentiated chordomas (DCs) are the most common. They almost exclusively occur as recurrent disease or after radiation therapy, appearing as the final evolution of an aggressive chordoma, while de novo cases are exceptional. The vast majority of reported DCs arose from the sacral region and only few from the skull base.[13-17] Additionally, data on molecular and genetic alterations leading to tumor dedifferentiation are missing.

Aim of this study was to better define typical pathological, radiological and clinical features, and to identify potential genetic alterations responsible for tumor dedifferentiation, in the largest series of skull base DCs treated surgically in a referral Center and for which detailed pathologic description was available.

MATERIALS AND METHODS

All subsequent cases of skull base DCs operated at our Center with endoscopic endonasal surgery between January 1990 and June 2019 were retrospectively evaluated. Clinical and radiological data, as well as information on the type and outcome of surgery and other adjuvant treatments, were retrieved from patient paper and electronic records. All patients underwent clinical and magnetic resonance imaging (MRI) examination 3 months after surgery, then every 6-12 months, depending on disease evolution.

According to the current World Health Organization 'Classification of Tumors of Soft Tissue and Bone', diagnostic criteria for the definition of DC was the presence of a biphasic tumour made of a portion with conventional chordoma cells juxtaposed to another with high-grade undifferentiated cell tumor or osteosarcoma cell features [1].

The study was approved by an inter-hospital Ethical Committee of Bologna city (ID # 585/2018/Oss/AOUBo). Written informed consent for the use of sensitive data was obtained from all

patients after detailed explanation of the purpose and nature of the study.

Immunohistochemical analysis

Tumor specimens, collected during surgery, were fixed in 10% formalin, embedded in paraffin and stained with hematoxylin and eosin (H&E). Immunohistochemical analysis was performed using commercially available antibodies, including S-100, clone 4C4.9 (Roche-Ventana); pan-cytokeratin, clone AE1/AE3/PCK26 (Roche-Ventana); epithelial membrane antigen (EMA), clone E29 (Roche-Ventana); INI1 (also known as SMARCB1), clone MRQ-25 (Roche-Ventana, Tucson, AZ); SATB2, Mouse Monoclonal antibody SATBA4B10 (Santa Cruz Biotechnology, 1:200 dilution); smooth muscle actin, Monoclonal antibody 1A4, prediluited (Ventana); desmin, Monoclonal antibody DE-R-11, prediluted (Ventana); h-caldesmon, Monoclonal antibody h-CALD, prediluted (Ventana); myogenin, Monoclonal antibody EP162, prediluted (Roche-Ventana); and Brachyury (H-210): sc-20109 (Santa Cruz Biotecnology). All sections were stained using Ventana automated stainer benchmark ULTRA IHC system. Blind review of all tissue slides was performed by three expert pathologists (CR, AR and SA).

Mutation analysis

Three sections of 10 μm each were cut and DNA from macro-dissected tumor tissue was digested at 56 °C for three hours using the Quick ExtractTM FFPE DNA extraction kit (Epicentre, Madison, WI, USA), as previously described.[18] *KRAS* (exons 2–4), *NRAS* (exons 2–4), *HRAS* (exons 2, 3), *BRAF* (exon 15), *PIK3CA* (exons 10, 21), *TP53* (exons 4–9), *NOTCH1* (exons 4, 6, 11, 26, 27), *PTEN* (exons 5–8), *CDKN2A* (exons 1, 2) and *EGFR* (exons 18–21) gene were evaluated by Next Generation Sequencing (NGS), as previously described.[19] These genes were chosen based on previous studies showing their alterations in chordomas.[20-22] In brief, target-specific amplicon libraries were generated using two steps PCR with overhang adapters based on the 5' Nextera sequences. The amplification products of the first target enrichment step were purified and employed as templates in the second (barcoding) PCR step (8 cycles). The barcoded amplicons were purified using MagSi-NGSPREP beads, quantified, pooled, and loaded onto a MiSEQ platform (Illumina). FASTQ files were processed in a Galaxy Project environment for quality check (PHRED quality

score >Q30, and length >100 bp), and for mapping and variant analysis using Bowtie 2.[23] PCR duplicates were excluded with the Picard MarkDuplicates tool (Broad Institute, Cambridge, MA). Quality score recalibration and regional realignment were determined with the Genome Analysis Toolkit (GATK 2.8; Broad Institute). Integrative Genomic Viewer (IGV) was used to identify all mutations of a clinical sensitivity threshold >5%; only bidirectional variant calls with more than 10 reads were reported. Mutations found were verified on COSMIC database (https://cancer.sanger.ac.uk/cosmic).

Methylation analysis

Bisulfite treatment of genomic DNA was performed using the EZ DNA Methylation-Lightning™ Kit (Zymo Research, cod. D5031) according to the manufacturer's protocol. DNA methylation analysis was performed by bisulfite-NGS for *BRCA1, BRCA2, PDCD1, PD-L1, CDH1, PRC1, MAGEA2, MAGEA11, TERT* and *UXT* gene, as previously described.[24] Briefly, a two-step library was prepared following the same protocol described above for mutation analysis. FASTQ files were processed for quality control (PHRED quality score >Q30) and for read lengths (>100 bp), then converted into FASTA format in a Galaxy Project environment.[23] To evaluate the methylation ratio of each CpG, FASTA files were loaded into the bisulfite sequencing pattern analysis tool (BSPAT-http://cbc.case.edu/BSPAT/index.jsp).[25] Methylation plotter (http://gattaca.imppc.org:3838/methylation_plotter/) was used to evaluate differences in methylation level between the group of classical and dedifferentiated chordomas.[26]

Statistical analysis

Survival of patients with classic and dedifferentiated chordomas was compared using Kaplan-Meier curves and log-rank test.

RESULTS

Clinical and radiological features

Six (4 F) out of 85 chordomas treated surgically at our Institution were identified, on the basis of

morphology and immunohistochemistry, as DCs. Mean age at surgery was 46 years (range 35-64; Table 1). Three out of 62 patients treated with surgery and radiation therapy developed DC (mean latency time 13.6 years from diagnosis; range 5-25). Other two patients developed DC after incomplete surgical resection of a typical chordoma, while one was "de-novo" or treatment-naïve. The last three cases received proton beam therapy after surgery.

The most commonly reported symptom at diagnosis was diplopia due to VI cranial nerve palsy (5 cases), that was associated with dysphagia and hemiparesis due to brainstem compression in one patient. One patient presented with dysphagia due to lower cranial nerves deficit.

The tumor was located in the upper third of the clivus in 4 cases, and involved the entire clivus in two. All tumors were extradural with intradural extension in 2 cases. At pre-operative MRI, 5 cases presented with dishomogeneous pattern in T2-weighted images, and non-homogeneous post-contrast enhancement in T1-weighted images, corresponding to the two different portions of the tumor (Figure 1).

At surgery, tumor usually presented with bone erosion, corresponding to the conventional chordoma pattern at histological examination, and a firm elastic component with strict adherence or infiltration of surrounding neurovascular structures (i.e. carotid artery), histologically corresponding to the dedifferentiated part of the tumor. Due to technical limitations, gross total removal could not be achieved and surgery was stopped in correspondence with the more fibrous portion of the tumor to avoid complications or permanent neurological sequelae. Subtotal tumor removal with a tumor remnant <20% of the initial mass was achieved in 3 cases, while in the others only partial tumor removal with a remnant >20% of the initial mass was possible. The most relevant surgical complication was internal carotid artery injury that occurred at the genu between petrosal and paraclival tracts in one case due to vessel infiltration by the dedifferentiated part of tumor, causing bleeding during dissection maneuvers. The carotid artery was occluded by an endovascular procedure with no neurological sequelae for the patient.

Mean follow-up was 31 months (range 11-52). Five out of 6 patients died for tumor progression. Mean survival time was 29 months (range 11-52 months) from DC diagnosis. The remaining patient presented a consistent progression of the remnant after 12 months, requiring a second surgery that was performed using the same approach. Neurological deficits were stable after

surgery and the patient was alive with disease at last follow-up, performed 34 months after DC diagnosis.

Pathological features

Histological examination confirmed the presence of two distinct components, observed at pre-operative MRI (Figure 1) and during surgery. Since intracranial specimens were mostly summited for pathological diagnosis in a piecemeal fashion, the two different components were not easily recognized on the microscope in the same fragment. Despite this, a morphological and immunohistochemical diagnosis of DC was done in all cases, showing a portion with features typical of conventional chordoma, juxtaposed to a dedifferentiated portion without notochordal differentiation. The two tumor portions were well demarcated, with an abrupt change between them (Figure 2).

In particular, in conventional chordoma areas, clusters or cords of medium to large plump cells with abundant lightly basophilic to clear cytoplasm containing small and large vacuoles (physaliferous cells) against a chondromyxoid intercellular matrix were evident. In the 3 patients developing DC after surgery and radiotherapy for conventional chordomas (cases 1, 2 and 3), the conventional chordoma component was focal and showed signs of tumoral necrosis and fibrosclerosis in the majority of the neoplastic tissue examined, even if few viable physaliferous cells in a chondromyxoid matrix were evident. In the two recurrent cases (cases 4 and 5), physaliferous cells atypia was more pronounced as compared with the primary conventional chordoma. Immunohistochemically, conventional chordoma cells were positive for brachyury and epithelial markers, including pan-cytokeratin and EMA. The dedifferentiated component was formed by spindle or pleomorphic cells with atypical spindle or oval nuclei and poorly defined cell boundaries, arranged in short fascicles. Based on the high tissue cellularity and mitotic figures (>20 mitoses/10 high power field), as well as the presence of foci of tumoral necrosis, diagnosis of high-grade pleomorphic sarcoma was done in three cases, and of high-grade spindle cell sarcoma in the remaining ones. Immunohistochemically, these spindle or pleomorphic tumor cells were negative for all the above-mentioned markers of conventional chordoma (i.e. brachyury, S-100 protein, pan-cytokeratin and EMA), muscle tissue markers (i.e. smooth muscle actin, desmin, h-caldesmon and myogenin). Osteogenic marker SATB2.

SMARCB1/INI1 was preserved in both tumour components in all cases.

Patients with DCs showed an earlier decline in survival when compared to patients with conventional chordomas, but after 12 years from diagnosis the two curves were approaching. The log-rank test was not significant (χ^2=1.24, p=0.266), although the small number of events among the group of DCs limits the robustness of this finding.

Genetic features

The mutation and methylation analyses of the two different components were feasible in two cases (cases 4 and 6) because of poor DNA quality in the other 4 (DNA was extracted from formalin-fixed, paraffin-embedded decalcified bone tumour tissue). Case 6, corresponding to the treatment-naïve DC, presented a mutation in *PIK3CA* (p.E542K; VAF (Variant Allele Frequency): 25%; COSM29329) in both tumour components. Another case treated with surgery and radiation therapy showed the *TP53 p.P151L* (VAF: 15%, COSM44288) mutation in the dedifferentiated tumour component. No mutations were found in the other case. DNA methylation analysis performed in the dedifferentiated tumour component revealed a tendency toward lower level of DNA methylation in three key genes: *MAGEA11* (Figure 3A)*, TERT* (Figure 3B) and *UXT* (Figure 3C) in both of the analyzed cases. No significant differences in DNA methylation were detected for in the genes *CDH1, BRCA1, BRCA2, PDCD1, PD-L1, PRC1* and *MAGEA2*.

DISCUSSION

Skull base DCs are very rare and, to our knowledge, only 17 cases have been reported in literature (Table 2).[5,6,13,15,16] Pathognomonic features and etiopathogenesis remain incompletely defined for the lack of large case series.

We presented the largest series with detailed pathologic description in literature made of 6 skull base DCs treated surgically at a single referral Center, to depict the main pathological (i.e. histological and molecular), clinical and radiological features, together with their outcome.

All DCs occurred in adults with a slight female predominance, typically during tumor progression of conventional chordomas after several years from surgery and radiation therapy (50% of the cases).

In all tumors, a double component could be identified at radiological examination and surgical inspection, that was confirmed at histologically, demonstrating peculiar morphological, immunohistochemical and molecular features.

In contrast with sacrococcygeal chordomas, skull base chordomas cannot be removed en-bloc for their invasive nature and critical anatomical location, i.e. proximity to vital neurovascular structures.[17,27,28] It has been recently reported that chordoma dedifferentiation significantly reduced the rate of gross total resection,[29] since their firm and teso-elastic consistency made radical resection quite impossible to achieve, independently from the surgical approach, as confirmed by our experience.

Furthermore, DCs are more resistant to radiation therapy as compared to other histological chordoma subtypes of, as demonstrated by fatal tumor progression in 5 of the 6 cases of our series. Similarly, Kayani et al. reported local tumor recurrence in 6 out of 7 patients (85.7%) treated with adjuvant radiotherapy (20–70 Gy) in a case series of 10 dedifferentiated sacral chordomas, while Kato et al. showed tumor recurrence just 4 months after carbon-ion radiotherapy in a dedifferentiated sacral chordoma.[12,14] According to our data, DCs typically occurred after radiation therapy (50%) or recurrence of conventional chordomas (33% of the cases), a finding that supports the hypotheses formulated on their pathogenesis, including radiation-induced malignant transformation or spontaneous progression of a single tumor.[8-12]

The detection of the same identical *PIK3CA* mutation in the two tumour portions in one case supports the hypothesis of tumour monoclonal origin. A previous study aimed at assessing genetic mutations in 10 conventional chordomas detected a loss of 3q26.32 (*PIK3CA*) in all tumors, suggesting the potential role of the PI3K pathway in chordoma development.[29] Recently, the importance of PI3K signaling mutations in these tumours has been confirmed by Tarpey et al. who demonstrated the presence of driver events in PI3K signaling genes in 17 out 104 (16%) sporadic chordomas and speculated on the utility of targeting PI3K signaling in their treatment.[30] Additionally, in another case we detected a mutation in *TP53* and epigenetic aberrations in *TERT, UXT* and *MAGEA11*, belonging to the larger family of cancer/testis antigens, whose expression is consistently detected in cancers of different histological origin and germinal cells.[31-33] On the other hand, *TP53* mutation associated with p53 immunohistochemical overexpression has been reported in the

sarcomatous component of four dedifferentiated chondrosarcomas and in dedifferentiating thyroid carcinomas.[34,35]

With regard to clinical outcome, DC is associated with an aggressive clinical course and poor prognosis, since 5 out of 6 patients died from disease progression soon after the detection of tumor dedifferentiation (mean 29 months). The remaining patient was still alive but with active disease after 34-month follow-up. In a study by Wu et al., 8 out of 106 patients with skull-base chordomas presented with DCs. Tumour dedifferentiation occurred after a mean of 37.1 months from the first surgical treatment and overall 5-year survival rate was 25%.[6] nOuyang et al. identified 6 DCs in a series of 77 skull base chordomas. Overall survival rate and progression-free survival were of 60% at 3-year follow-up.[5] The main limitation of the above-mentioned largest case series is the lack of morphological and immunohistochemical description.

Morphologically, DCs have to be differentiated from the two others aggressive chordoma variants, i.e. sarcomatoid and poorly differentiated, representing a challenging task for the pathologist (Table 3). In particular, the similar clinical presentation and the presence of a sarcomatous component - made of pleomorphic or spindle cell sarcoma or, rarely, osteosarcoma - observed in a recurrent or initial tumor after radiation therapy make differential diagnosis between DC and sarcomatous chordoma difficult. The presence of a transitional feature between the conventional chordoma and the sarcomatous component, and the immunoreactivity for brachyury, pan-cytokeratin and/or EMA in both tumour components allow to distinguish this aggressive chordoma variant - also reported in literature as chordoma with predominant spindling of the epithelial cells" or "sarcomatoid chordoma" -, from DC.[9,11,13,17] Conversely, poorly differentiated chordoma has a distinct clinical, morphological and immunohistochemical profile compared to DC. The typical clinical presentation in children, the recurrent deletions encompassing the SMARCB1 locus - resulting in consistent loss of nuclear immunoexpression of SMARCB1/INI1 associated with sheets of epithelioid cells with nuclear pleomorphism -, the abundant eosinophilic cytoplasm, and the increased number of mitoses without dedifferentiation areas are the most important features to distinguish this variant from DC.[7,8] Finally, clinical history, radiographic and morphological findings associated with a strong nuclear expression of brachyury antibody in the neoplastic cells of conventional chordoma areas of DC are essential for differential diagnosis with metastatic carcinoma.

Points of strength of this study are the large number of cases included in the series, the homogeneous surgical treatment, as well as radiological and pathological characterization, performed in a unique referral Center. Moreover, for the first time, critical genetic aberrations potentially underlying the dedifferentiation process were investigated. Main limitation is represented by the retrospective design.

In conclusion, the transformation of a conventional chordoma into a dedifferentiated tumor is a rare event, that typically occurs at recurrence or after radiation therapy. The presence of a dedifferentiated tumor component dramatically reduces the chance of cure. Therefore, early detection is fundamental. Pre-operative MRI could be useful at this purpose due to the presence of suggestive features of dedifferentiation. Further studies including a larger number of cases with complete radiological and clinic-pathological profile, including molecular investigation, are strongly encouraged to improve the knowledge on chordoma pathobiology, and to potentially identify early reliable predictors of dedifferentiation, outcome and of response to treatment.

Acknowledgments

This work was supported by the research grant "Ricerca Fondamentale Orientata (RFO)" to Dr. Sofia Asioli. Funding sources did not influence the study design, nor the collection, analysis and interpretation of data, the writing of the report and the decision to submit the article for publication. All authors contributed to the study conception and design. Tissue preparation for histological analysis, DNA extraction and analysis, data collection and analysis were performed by Costantino Ricci, Giacomo Sollini, Federica Guaraldi, Matteo Zoli and Diego Mazzatenta. The first draft of the manuscript was written by Sofia Asioli and Alberto Righi. All authors contributed to improve manuscript and approved its final version.

References

1. Flanagan A, Yamaguchi T (2013) Notochordal tumours. In World Health Organization Classification of Tumours of Soft Tissue and Bone, IARC Press: Lyon; 326-329.

2. Bakker SH, Jacobs WCH, Pondaag W et al. Chordoma: a systematic review of the epidemiology and clinical prognostic factors predicting progression-free and overall survival. Eur Spine J 2018; 27(12): 3043-3058.

3. Righi A, Sbaraglia M, Gambarotti M et al. Extra-axial chordoma: a clinicopathologic analysis of six cases. Virchows Arch 2018; 472(6): 1015-1020.

4. Tsukamoto S, Vanel D, Righi A, Donati DM, Errani C. Parosteal extra-axial chordoma of the second metacarpal bone: a case report with literature review. Skeletal Radiol 2018; 47(4): 579-585.

5. Ouyang T, Zhang N, Zhang Y et al. Clinical characteristics, immunohistochemistry, and outcomes of 77 patients with skull base chordomas. World Neurosurg 2014; 81(5-6): 790-797.

6. Wu Z, Zhang J, Zhang L et al. Prognostic factors for long-term outcome of patients with surgical resection of skull base chordomas-106 cases review in one institution. Neurosurg Rev 2010; 33(4): 451-456.

7. Hasselblatt M, Thomas C, Hovestadt V et al Poorly differentiated chordoma with SMARCB1/INI1 loss: a distinct molecular entity with dismal prognosis. Acta Neuropathol 2016; 132: 149-151.

8. Shih AR, Cote GM, Chebib I et al. Clinicopathologic characteristics of poorly differentiated chordoma. Mod Pathol 2018; 31(8): 1237-1245.

9. Morimitsu Y, Aoki T, Yokoyama K, Hashimoto H. Sarcomatoid chordoma: chordoma with a massive malignant spindle-cell component. Skeletal Radiol 2000; 29(12): 721-725.

10. Tomlinson FH, Scheithauer BW, Forsythe PA, Unni KK, Meyer FB. Sarcomatous transformation in cranial chordoma. Neurosurgery 1992; 31: 13–18.

11. Miettinen M, Karaharju E, Järvinen H. Chordoma with a massive spindle-cell sarcomatous transformation. A light- and electron-microscopic and immunohistological study. Am J Surg Pathol 1987; 11(7): 563-570.

12. Kayani B, Sewell MD, Hanna SA et al. Prognostic factors in the operative management of dedifferentiated sacral chordomas. Neurosurgery 2014; 75(3): 269-275.

13. Frankl J, Grotepas C, Stea B, Lemole GM, Chiu A, Khan R. Chordoma dedifferentiation after proton beam therapy: a case report and review of the literature. J Med Case Rep 2016; 10: 280.

14. Kato S, Gasbarrini A, Ghermandi R, Gambarotti M, Bandiera S (2016) Spinal chordomas dedifferentiated to osteosarcoma: a report of two cases and a literature review. Eur Spine J 2016; 25 Suppl 1: 251-256.

15. Hara T, Kawahara N, Tsuboi K, Shibahara J, Ushiku T, Kirino T (2006) Sarcomatous transformation of clival chordoma after charged-particle radiotherapy. Report of two cases. J Neurosurg 105(1):136-141.

16. Rabade N, Goel N, Goel A. Clival dedifferentiated chordoma: a case report. Anal Quant Cytopathol Histpathol 2014; 36(6): 330-334.

17. Zorlu F, Gürkaynak M, Yildiz F, Oge K, Atahan I. Conventional external radiotherapy in the management of clivus chordomas with overt residual disease. Neurol Sci 2000; 21:203–207.

18. Gissi DB, Tarsitano A, Leonardi E et al. Clonal analysis as a prognostic factor in multiple oral squamous cell carcinoma. Oral Oncol 2017; 67: 131-137.

19. Gabusi A, Gissi DB, Tarsitano A et al. Intratumoral Heterogeneity in Recurrent Metastatic Squamous Cell Carcinoma of the Oral Cavity: New Perspectives Afforded by Multiregion DNA Sequencing and mtDNA Analysis. J Oral Maxillofac Surg 2019; 77(2):440-455.

20. Hallor KH, Staaf J, Jönsson G et al. (2008) Frequent deletion of the CDKN2A locus in chordoma: analysis of chromosomal imbalances using array comparative genomic hybridisation. Br J Cancer 98(2):434-442.

21. Choy E, MacConaill LE, Cote GM et al. Genotyping cancer-associated genes in chordoma identifies mutations in oncogenes and areas of chromosomal loss involving CDKN2A, PTEN, and SMARCB1. PLoS One 2014; 9(7):e101283.

22. Fischer C, Scheipl S, Zopf A et al. Mutation Analysis of Nine Chordoma Specimens by Targeted Next-Generation Cancer Panel Sequencing. J Cancer 2015; 6(10): 984-989.

23. Afgan E, Baker D, Batut B et al. The Galaxy platform for accessible, reproducible and collaborative biomedical analyses: 2018 update. Nucleic Acids Res 2018;_ 46(W1): W537-W544.

24. Morandi L, Gissi D, Tarsitano A et al. CpG location and methylation level are crucial factors for the early detection of oral squamous cell carcinoma in brushing samples using bisulfite sequencing of a 13-gene. Clin Epigenetics 2017; 9: 85.

25. Hu K, Ting AH, Li J. BSPAT: a fast online tool for DNA methylation co-occurrence pattern analysis based on high-throughput bisulfite sequencing data. BMC Bioinformatics 2015; 16: 220.

26. Mallona I, Díez-Villanueva A, Peinado MA. Methylation plotter: a web tool for dynamic visualization of DNA methylation data. Source Code Biol Med 2014; 9:11.

27. Zoli M, Milanese L, Bonfatti R et al. (2018) Clival chordomas: considerations after 16 years of endoscopic endonasal surgery. J Neurosurg 2018; 128(2): 329-338.

28. Doucet V, Peretti-Viton P, Figarella-Branger D, Manera L, Salamon G. MRI of intracranial chordomas. Extent of tumour and contrast enhancement: criteria for differential diagnosis. Neuroradiology 1997; 39:571–576.

29. Rinner B, Weinhaeusel A, Lohberger B, et al. Chordoma characterization of significant changes of the DNA methylation pattern. PLoS One 2013; 8: e56609.

30. Tarpey PS, Behjati S1, Young MD et al. The driver landscape of sporadic chordoma. Nat Commun 2017; 8(1): 890.

31. Wang Y, Schafler ED, Thomas PA et al. Prostate-specific loss of UXT promotes cancer progression. Oncotarget 2019; 10(7): 707-716.

32. Van Tongelen A, Loriot A, De Smet C. Oncogenic roles of DNA hypomethylation through the activation of cancer-germline genes. Cancer Lett 2017; 396:130-137.

33. Yuan X, Larsson C, Xu D. Mechanisms underlying the activation of TERT transcription and telomerase activity in human cancer: old actors and new players. Oncogene 2019; 38(34): 6172-6183.

34. Bovée JV, Cleton-Jansen AM, Rosenberg C, Taminiau AH, Cornelisse CJ, Hogendoorn PC. (1999) Molecular genetic characterization of both components of a dedifferentiated chondrosarcoma, with implications for its histogenesis. J Pathol 1999; 189(4): 454-462.

35. Nikiforova MN, Wald AI, Roy S, Durso MB & Nikiforov YE Targeted next-generation sequencing panel (ThyroSeq) for detection of mutations in thyroid cancer. J Clin Endocrinol Metab 2013; 98 E1852–E1860

Tables

Table 1. Main patient clinical features

N°	Age/ Sex	Previous Treatment	Pre-operatory symptoms	Time of tumor dedifferentiation after diagnosis (years)	Tumor removal	Outcome and time of follow-up (months)
1	35/M	S + RT	Ophthalmoplegia	5	STR	DOD; 20

2	55/F	S + RT	Hemiparesis, dysphagia, ophtalmoplegia	25	PTR	DOD; 11
3	40/F	S + RT	Ophthalmoplegia	11	STR	DOD; 52
4	64/F	Biopsy	Dysphagia	1	PTR	DOD; 40
5	35/F	Biopsy	Ophthalmoplegia	1	STR	AWD; 34
6	46/M	None	Ophthalmoplegia	0 ("de-novo")	PTR	DOD; 28

Legend to table: AWD: alive with disease; DOD: died of disease; F: female; M: male; PTR: partial tumor removal; RT: radiation therapy; S: surgery; STR: subtotal tumor removal

Table 2. Literature review of dedifferentiated chordomas of the skull base.

Author, year	**N patients included**	**Age (yr)/ Gender**	**Time of tumor dedifferentiation after diagnosis (months)**	**Outcome and follow-up duration**
Ouyang et al.[5]	6*	N/A	N/A	3-yr follow-up: 60% overall survival; 40% progression-free survival
Wu et al.[6]	8*	N/A	37.1 (mean)	5-years overall survival: 25%
Frankl et al.[13]	1	8 / F	30 (after proton-therapy)	AWD; 46 months
Hara et al.[15]	1	47 / F	60 (after carbon-ion therapy)	DOD; 62 months
Rabade et al.[16]	1	58 / M	60	AWD; 60 months

Legend to table: * histological description not available for every single case; AWD: alive with disease; DOD: died of disease; F: female; M: male

Table 3. Distinctive clinico-pathological features of the different aggressive chordoma variants

Feature	***Sarcomatous***	***Poorly differentiated***	***Dedifferentiated***
Age at presentation (mean and range)	**adult** (48 yr; 34-74 yr)	**children and adolescent** (9.3 yr; 3 m-42 yr)	**adult** (43.1 yr; 8-64 yr)
Gender distribution (F:M)	1:1	1.4:1	2:1
Typical site of onset	sacrococcygeal	skull base	sacrococcygeal
Microscopic features	Alternating cellular (proliferation of atypical spindle cells) and loose-looking (conventional chordoma) components	Epithelioid cells with prominent nuclear pleomorphism and relatively abundant eosinophilic cytoplasmic, and with a cohesive and often sheet-like pattern of growth	Biphasic tumor comprising the features of a conventional chordoma which was juxtaposed to a high-grade undifferentiated tumor
Chondromyxoid matrix and physaliphorous cells	present	absent in ≈80% of cases	present in conventional chordoma area

Gradual transition between conventional and sarcomatous component	present	absent	absent
Immmuhistochemistry			
Brachyury	+	+	**+ in conventional area** **- in dedifferentiated area**
Pan-cytokeratin	+/-	+	**+ in conventional area** **- in dedifferentiated area**
SMARCB1/INI1	N/A	**-**	**+ in conventional area** **+ in dedifferentiated area**
Prognosis	100% mortality; median survival 4 months	38% mortality; median survival 14 months	60% mortality; median survival 36 months

Figures Legend

Figure 1. T1-weighted MRI sequences after gadolinium administration, axial slice (case 4 of the series; see Table 1 for details). The two different neuroradiological patterns can be appreciated, corresponding to the different pathological components of the lesion. dedifferentiated portions present

homogenous and vivid post-contrast enhancement on T1-weighted images, while the conventional chordoma area of the tumor presents dishomogeneous post-contrast enhancement.

Figure 2. Tumor slices stained with hematoxylin and eosin, showing the different histological patterns associated with classical and dedifferentiated chordoma. A and B. Dedifferentiated chordoma consists of cells typical of classical chordoma juxtaposed to high-grade undifferentiated spindle and/or pleomorphic cells (B: 100X of magnification). C. Classical chordoma is made of physaliferous cells while dedifferentiated chordoma shows fascicular proliferation of undifferentiated spindle-or pleomorphic-shaped tumor cells (200X of magnification). D. Immunohistochemically, classical chordoma cells show nuclear positivity for brachyury, whose expression is lost in the spindle/pleomorphic cell dedifferentiated chordoma (200X of magnification).

Figure 3. Boxplots for each group of samples: a set of 15, 6 and 6 CpGs within the promoter of *MAGEA11, TERT, UXT* respectively, were investigated for DNA methylation level. Classic chordoma showed a mean value for *MAGEA11* of 0.380 in a range from 0.218 to 0.715; dedifferentiated component showed a mean value of 0.295, in a range from 0.140 to 0.526; *TERT* mean value was 0.915 (range from 0.793 to 0.974) for classic component and 0.834 (range from 0.658 to 0.905) for dedifferentiated one. *UXT* mean value was 0.307 (range from 0.197 to 0.335) for classical component and 0.213 (range from 0.166 to 0.230) for dedifferentiated one.

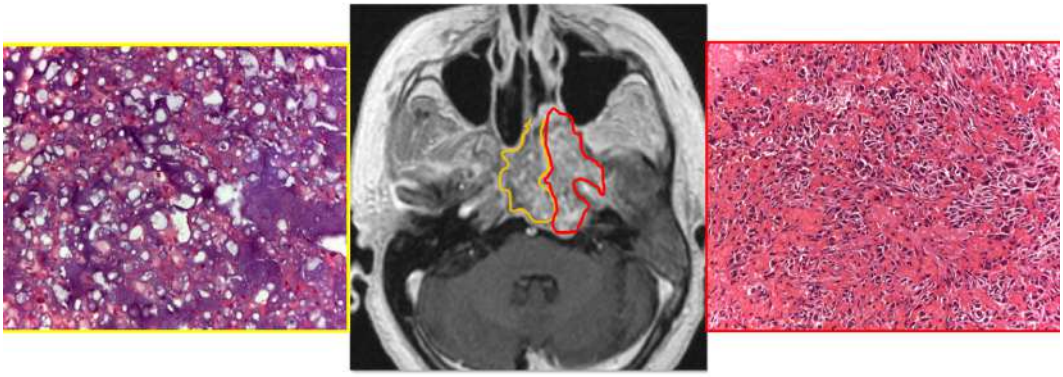

his_14024_f1.tif

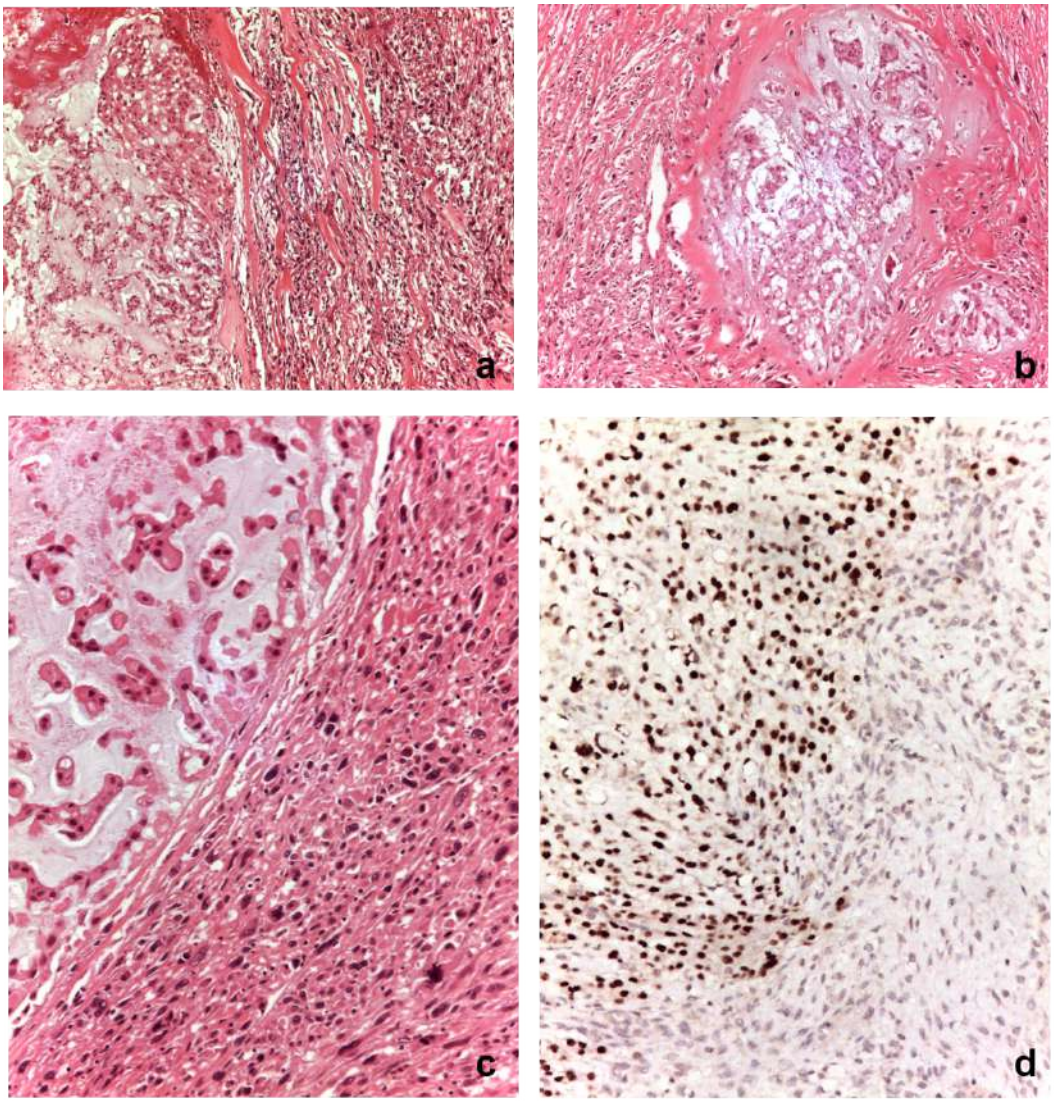

his_14024_f2.tif

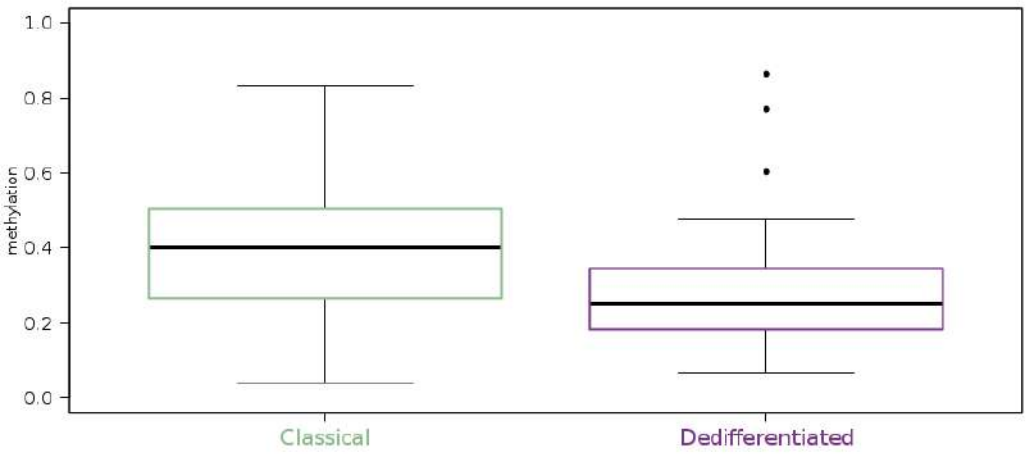

his_14024_f3a.tiff

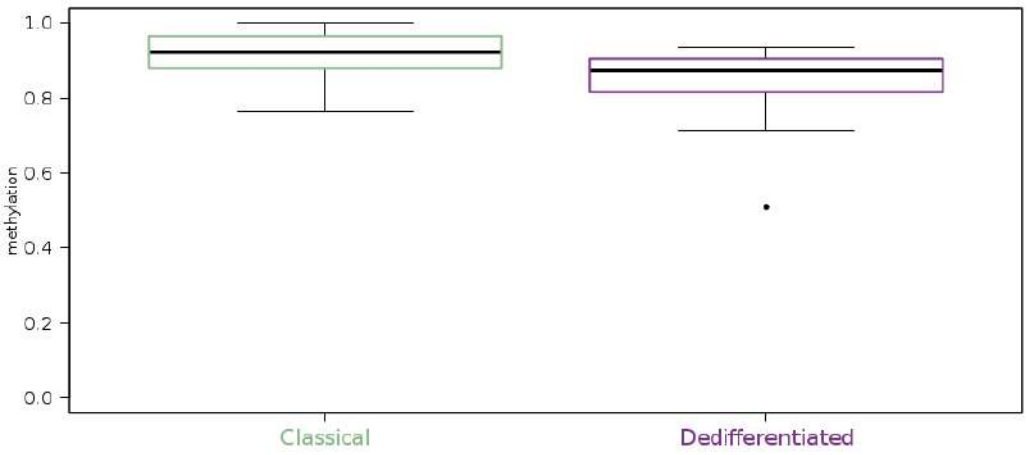

his_14024_f3b.tiff

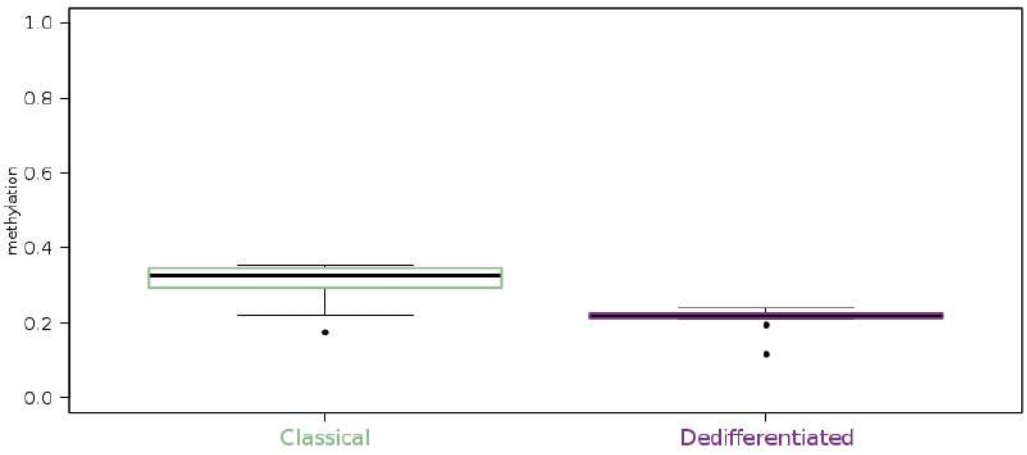

his_14024_f3c.tiff